

Article

Local-Scale Mapping of Biomass in Tropical Lowland Pine Savannas Using ALOS PALSAR

Dimitrios Michelakis ^{1,*}, Neil Stuart ¹, German Lopez ², Vinicio Linares ³ and Iain H. Woodhouse ¹

¹ School of Geosciences, College of Science and Engineering, University of Edinburgh, Edinburgh, EH8 9XP, UK; E-Mails: ns@staffmail.ed.ac.uk (N.S.); i.h.woodhouse@ed.ac.uk (I.H.W.)

² School of Environment Natural Resources and Geography, Bangor University, Bangor, LL57 2UW UK; E-Mail: glopez@ub.edu.bz

³ Forestry, Entrepreneurship, Finance and Corporate Social Responsibility, Greater New York City Area, USA; E-Mail: avlin14@gmail.com

* Author to whom correspondence should be addressed; E-Mail: dimmihel@gmail.com; Tel.: +44-131-650-9046; Fax: +44-131-650-2524.

Received: 3 April 2014; in revised form: 8 September 2014 / Accepted: 22 September 2014 /

Published: 25 September 2014

Abstract: Fine-scale biomass maps offer forest managers the prospect of more detailed and locally accurate information for measuring, reporting and verification activities in contexts, such as sustainable forest management, carbon stock assessments and ecological studies of forest growth and change. In this study, we apply a locally validated method for estimating aboveground woody biomass (AGWB) from Advanced Land Observing Satellite (ALOS) Phased Array-type L-band Synthetic Aperture Radar (PALSAR) data to produce an AGWB map for the lowland pine savannas of Belize at a spatial resolution of 100 m. Over 90% of these woodlands are predicted to have an AGWB below 60 tha^{-1} , with the average woody biomass of these savannas estimated at 23.5 tha^{-1} . By overlaying these spatial estimates upon previous thematic mapping of national land cover, we derive representative average biomass values of ~32 tha^{-1} and ~18 tha^{-1} for the previously qualitative classes of “denser” and “less dense” tree savannas. The predicted average biomass, from the mapping for savannas woodlands occurring within two of Belize’s larger protected areas, agree closely with previous biomass estimates for these areas based on ground surveys and forest inventories (error $\leq 20\%$). However, biomass estimates derived for these protected areas from two biomass maps produced at coarser resolutions (500 m and 1000 m) from global datasets overestimated biomass (errors $\geq 275\%$ in each dataset).

The finer scale biomass mapping of both protected and unprotected areas provides evidence to suggest that protection has a positive effect upon woody biomass, with the mean AGWB higher in areas protected and managed for biodiversity (protected and passively managed (PRPM), 29.5 tha^{-1}) compared to unprotected areas (UPR, 23.29 tha^{-1}). These findings suggest that where sufficient ground data exists to build a reliable local relationship to radar backscatter, the more detailed biomass mapping that can be produced from ALOS and similar satellite data at resolutions of ~ 100 m provides more accurate and spatially detailed information that is more appropriate for supporting the management of forested areas of $\sim 10,000$ ha than biomass maps that can be produced from lower resolution, but freely available global data sets.

Keywords: savanna woodlands; Earth observation; ALOS PALSAR; biomass map; conservation planning; Belize

1. Introduction

1.1. Why Map Tropical Savannas at More Local Scales?

Savannas are an important component of global vegetation, covering approximately 18% of the Earth's land surface [1]. The woody component of savannas can be variable [2]; however, many woody savannas can be characterized as forests according to the FAO definition [3]. The woody component is of major significance for storing biomass [4,5], supporting biodiversity [6] and sustaining the local hydrological cycle [7]. A growing recognition of the value of natural carbon stores and the intention to reduce emissions caused by deforestation and forest degradation [8] are encouraging developing countries to protect and manage these tropical forest ecosystems more sustainably.

Wooded areas within savannas are increasingly pressured by human intervention, leading to unsustainable management practices. In the Neotropics, key threats are the continuing expansion of agriculture and pasture [9,10], as well as overly frequent logging and burning [11,12], which have resulted in the reduced extent and health of this ecosystem [13,14].

With these pressures degrading both the biodiversity and economic value of savanna woodlands, techniques are urgently needed to measure, map and monitor the woody component reliably and to produce this information at appropriate scales to support conservation and management actions. Maps of aboveground woody biomass (AGWB), if sufficiently detailed, can assist conservation managers, practitioners and policy makers to formulate specific practices (e.g., thinning, fire control, seedling regeneration, biodiversity surveys, *etc.*) that are appropriate for woodland patches within broader savanna areas [15,16].

Many countries presently lack the capacity to produce their own local maps of forest biomass and, so, must rely on existing biomass maps founded upon broader regional and global datasets. Although providing a consistent approach to estimation of biomass differences over areas of hundreds of square kilometres, we contend that the resolution of these global data sets (typically 500 m or 1000 m) is often

too coarse for quantifying and monitoring the distribution of woody biomass within areas of 10,000 ha or less, which are common sizes for protected areas or forest reserves, particularly in smaller countries.

In this paper, we use the example of pine woodlands in Belize, for which a locally modelled relationship between ground measured biomass and satellite sensed radar backscatter from PALSAR has been established and validated, to explore finer scale biomass mapping to support potential forestry applications. Specifically, we address the following objectives:

- Mapping the AGWB of over 50% of the lowland savanna woodlands of Belize at 100-m resolution, using a locally modelled relationship between the satellite radar backscatter and observations of biomass from an extensive national inventory of forest plots.
- Analysing the resulting AGWB map to quantify for the first time the variation in AGWB across the different woodland savannas within the country and exploring how this might provide forest managers with enhanced information about the nature and locality of different woodland components, compared to previous qualitative thematic mapping using the UNESCO land cover classification system.
- Examining, within a pilot study area of approximately 933 km², whether the biomass map produced at 100 m might enable differences in biomass to be observed between forest areas that are being protected or sustainably managed, compared to unprotected forest areas.
- For two specific protected areas of Belize, assessing if this finer scale mapping produces biomass estimates that accord more closely with ground measurements of biomass than estimates based on biomass values extracted from pantropical biomass data sets at 500-m and 1000-m resolution produced by [17,18].

1.2. Mapping of Savanna Woodlands with Active Satellite Earth Observation

New advances in the mapping of biomass by active sensors have greatly facilitated efforts to characterize savanna ecosystems at multiple scales. Using the archive of the Advanced Land Observing satellite (ALOS) Phased Array-type L-band Synthetic Aperture Radar (PALSAR) satellite data collected from 2007–2009, the Japanese Aerospace Exploration Agency (JAXA) produced the first 50-m global forest/non-forest map [19] to support activities for the United Nations-Reducing Emissions from Deforestation and Degradation (UN-REDD+), while the Jet Propulsion Laboratory (JPL) in collaboration with JAXA created a regional mosaic of ALOS PALSAR imagery for wide ground swaths (~350 km) to assist ecosystem assessments in the Americas. Recent research has shown that ALOS PALSAR data are suitable for classifying vegetation types and assessing carbon stocks at regional scales [20]. In [17,18], satellite LiDAR measurements collected by Ice, Cloud, and land Elevation/Geoscience Laser Altimeter System (ICESAT GLAS), and a diversity of optical spaceborne sensors were used in combination with field measurements to create pantropical carbon stock maps with the explicit intent of assisting tropical countries with monitoring and reporting of their carbon stocks for UN-REDD+ projects at national and sub-national scales (*i.e.*, 10,000 ha). In Africa, [21] created an ALOS PALSAR mosaic at 100-m spatial resolution to be used, among other applications, to map deforestation and agricultural encroachment upon the forest-savanna boundary. In their study within savanna landscapes, [22] identified strong relationships between AGWB and radar backscatter sensed by ALOS PALSAR, concluding that the approach was necessary and sufficient for monitoring

and reporting of biomass baselines for REDD+ projects, and [23] similarly found ALOS PALSAR images to assist in quantifying deforestation at small scales in savanna woodlands in Mozambique. In Australia, [24] stressed the value of ALOS PALSAR data for quantifying the contribution of the woody component of tropical savannas to regional carbon stocks.

There is thus a growing body of evidence derived by studies conducted in tropical savannas supporting the technique of deriving biomass maps from L-band data collected by ALOS PALSAR, with the majority of the work to date conducted in African and Australian savannas. The wide availability of L-band data (up until 2011) and new L-band data acquisitions from operational ALOS PALSAR-2 (launched in 2014), as well as future spaceborne and airborne missions, such as the Satélite Argentino de Observación Microondas (SAOCOM) and NASA's airborne Unmanned Aerial Vehicle (UAV) SAR, makes it an attractive data source for wide and local area biomass monitoring. However, finer scale biomass mapping using L-band SAR data relies on establishing a strong and consistent relationship between the backscattered signal and biomass measurements collected in the field in each locality. The relationship between biomass and backscatter is known to vary for different woodlands and to be influenced by local topographic and climatic conditions, which, for example, affect the attenuation of the signal [25]. For these reasons, some attempts to create fine-scale biomass maps from ALOS PALSAR data have not been successful. For example, [26] were not able to map AGWB in savanna woodlands sufficiently accurately in Malawi, because of substantial topographic relief in the study area, combined with the heterogeneity of the woody component.

1.3. The Use of More Detailed Mapping of Woody Biomass in Savannas

Work is now progressing beyond dichotomous mapping of forest *versus* savanna, to create finer scale mapping of biomass differences within savanna landscapes. This is often driven by the need to create baseline carbon stock maps and to monitor changes in biomass as part of the reporting requirements of REDD+ projects. Although radar techniques are well established for mapping biomass in more uniform forest plantations, such as those in temperate and boreal regions, forest managers and researchers are raising questions about whether coarse resolution (*i.e.*, 500-m and 1000-m pixel resolution) mapping from EO data is adequate for tasks, such as primary production planning or forest stock mapping, in more heterogeneous woody environments, such as tropical savannas. For example, Jantz *et al.* in [27] used the 500-m biomass maps produced by [17] to plan corridors to connect together broadleaf forest areas and have suggested that a similar method could be used to identify conservation corridors in lower biomass ecosystems. Whilst the AGWB maps produced by [17,18] may be used to meet regional-scale emissions reporting requirements or for preliminary estimation of national carbon stocks when no finer scale information is available, these maps need to be validated against local forest stock surveys or AGWB maps from higher resolution satellite imagery when these are available.

Beyond the present focus on carbon stocks, there is wider interest in how finer scale spatial information about biomass in savanna woodlands can inform work in forest management and forest ecology. Biogeographers and forest ecologists studying shifts in savanna-forest boundaries can use finer scale information to detect changes in the relative balance between woody vegetation and grasses more rapidly, whilst finer scale data allows them to understand the relative importance of human

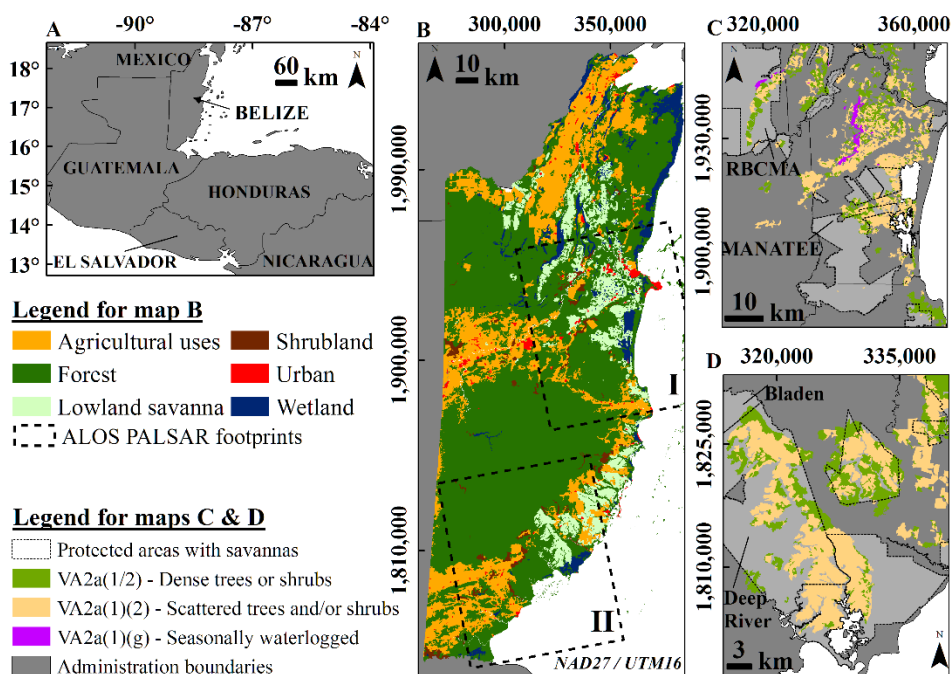
activities compared to climatic changes as factors influencing local shifts [4,28–33]. AGWB estimates derived from ALOS PALSAR may enable scientists to explore and monitor these dynamic phenomena and processes in more depth. There is also interest in using finer scale biomass mapping to monitor regeneration and growth in low density woodlands. For example, ALOS PALSAR data have been combined with Landsat data by [34,35] to characterize re-growth in open Brigalow woodlands in Australia to assist management strategies, such as thinning and weed control, illustrating practical management actions that can be supported by this finer scale information.

2. Experimental Section

2.1. Description of the Lowland Savanna Ecosystem

This study is conducted within the lowland areas of Belize (Figure 1A), which comprise approximately 1754 km² of savanna landscape [36] (Figure 1B). These areas are the most northern Neotropical savannas [37], which represent the second most extensive savanna vegetation formation within the America Neotropics [38]. In this analysis, we focus on mapping the aboveground woody biomass (AGWB) of woody savannas, which are recognized for their importance in carbon sequestration due to the presence of pine trees [39]. Pine (*Pinus caribaea* var. *hondurensis*) forms low density wood clusters (10%–65% canopy cover) within the savanna landscape, while other woody vegetation, such as Palms (*Acoelorrhaphe wrightii*) and shrubs (*Byrsonima crassifolia*), are often evident and usually scattered through the grass landscape [40].

Figure 1. (A) Belize in the region of Central America; (B) footprints of the ALOS PALSAR and the national ecosystems map based on UNESCO classes; and (C,D) the lowland savanna areas in the ALOS PALSAR scenes; light grey areas indicate the extent of protected areas with lowland savannas; RBCMA stands for Rio Bravo Conservation and Management Area.



The national ecosystems map of Belize classifies the lowland savannas into three UNESCO classes (Figure 1C and Figure 1D). Here, we examine the: (1) short-grass savannas with dense trees or shrubs (UNESCO code: VA2a (1/2)) (Figure 2A,C); and (2) short-grass savannas with scattered trees and/or shrubs (UNESCO code: VA2a (1) (2)) (Figure 2B,D). Pine woodlands occur in both of these vegetation zones, and the local density of the tree cover in relation to other shrubs and grasses has until now been interpreted qualitatively as the basis for allocating most savanna land into one or the other of these classes [41]. The climate in Belize is subtropical to tropical with an average annual precipitation of around 1500 mm in the northern parts of the country and 3800 mm in the south. In Figure 3, the annual mean precipitation is shown per month using data collected in three weather stations of the Belize National Meteorological Service and a rainfall monitoring product, which is based on derived data from the Global Precipitation Climatology Centre (GPCC).

Figure 2. Representative photographs of lowland savanna areas with dense trees or shrubs (VA2a (1/2)) (A,C); and sparse trees and/or shrubs (VA2a (1) (2)) (B,D).

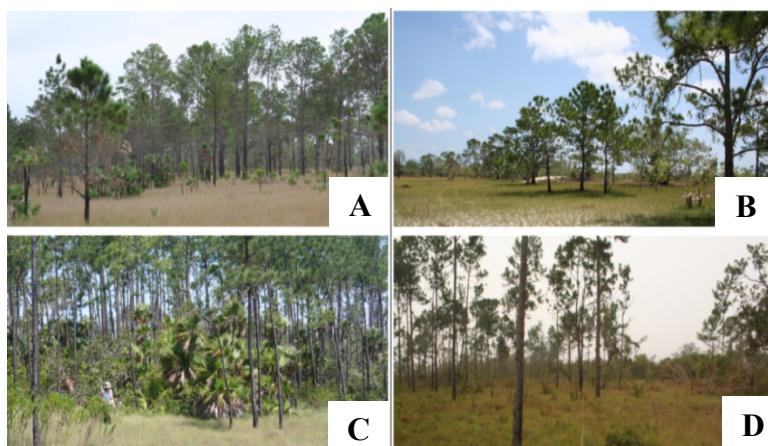
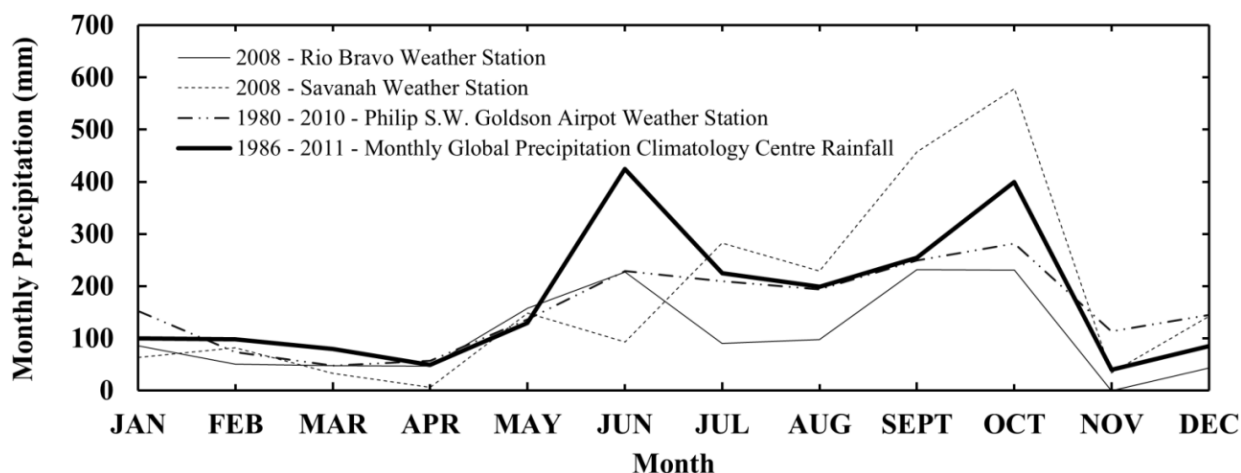


Figure 3. Illustrating the wet and dry seasonality in Belize; two major precipitation spikes are observed in June and October, while September also appears to be a rainy month.



2.2. ALOS PALSAR Data

Two fine beam dual polarization (FBD) ALOS PALSAR datasets (Level 1.0) covering approximately 55% (933.46 km²) of the lowland savanna ecosystem in Belize were collected during the wet season in September, 2008 (Figure 1B, I,II). The radar data that were used in this study included only the horizontal-vertical polarization (HV), because of their sensitivity to biomass found for the same areas used in this study in [42,43]. The HV data were pre-processed at Aberystwyth University from raw data to single look complex (SLC) images using the Modular SAR processor in GAMMA software, while a calibration factor of −58.30 decibels (dB) was used. Subsequently, the SLC images were multi-looked and geo-coded to precision images (PRI) using the differential interferometry geocoding module (DIFF and GEO), which is also included in GAMMA. The resulting four look images (pixel spacing ≈ 13 m) were further processed to reduce speckle by aggregating neighbourhoods of adjacent pixels (2 × 2) and arithmetically averaging the radar intensity at the power domain [42,43]. The final radar product has a pixel-spacing of 26 m, and data represent the normalized radar cross-section (σ_{dB}^0), where dB is decibels. The total extent of the lowland savanna has been mapped by previous projects [36], and that map is used to constrain the biomass mapping from the ALOS data to within the savanna extents.

The total study area is 933.46 km² (Figure 1, C,D) and is comprised of approximately 345 km² of lowland savannas with sparse trees or shrubs (VA2a (1/2) (51% of total VA2a (1/2))) and 588 km² of lowland savannas with dense trees or shrubs (VA2a (1) (2) (58% of total VA2a (1) (2))).

Although the ALOS PALSAR data were acquired during the wet season, the rainfall estimates of the Tropical Rainfall Measurement Mission (Product 3B42V7) for the radar data acquisition dates (+/− three days) within the study area shows that the mean rainfall is very low in both ALOS PALSAR images (~15 mm/day for Image I and ~9 mm/day for Image II). When comparing these mean precipitation estimates to the mean dry season gauged precipitation data acquired in the two weather stations falling within the ALOS PALSAR image extents (Figure 3), we have more confidence for using this ALOS PALSAR imagery, which was collected during the wet season for AGWB estimation.

2.3. Biomass Mapping Using ALOS PALSAR and Semi-Empirical Modelling

Biomass mapping was achieved by adapting a forward parametric model, which is based on a semi-empirical water cloud model (WCM) [42–44] to derive a mathematical relationship between the backscattered intensity of the radar signal (σ_{pp}^0), where *pp* corresponds to emitted and received polarization of the radar signal and the biomass (AGWB) calculated from ground surveys of 6,457 trees collected over 32.6 hectares of savanna woodlands throughout Belize.

In the WCM, the AGWB is represented as a relatively homogeneous aboveground volume, which consists of canopy components and air [42,44]; the canopy components are assumed to be relatively homogeneous spherical scatterers, which mimic a water cloud. Mathematically, the parametric forward model describing the WCM usually takes the form of Equation (1) to perform fitting, non-linear least squares regression and calculation of the empirical coefficients σ_{veg}^0 , σ_{soil}^0 and γ , which are dependent on the structure of the woodlands. The regression equation is then re-arranged to estimate biomass as shown in Equation (2) [42].

$$\sigma_{total}^0 = \sigma_{veg}^0 \times (1 - e^{(-\gamma \times AGWB)}) + \sigma_{soil}^0 \tag{1}$$

$$AGWB = \log_{\gamma} \left(\frac{\sigma_{soil}^0 - \sigma_{total}^0 + \sigma_{veg}^0}{\sigma_{veg}^0} \right) \tag{2}$$

In Equation (2), σ_{total}^0 represents the total backscattered intensity of the radar signal collected by ALOS PALSAR, σ_{veg}^0 is the fraction of the total backscattered intensity due to radar-vegetation interaction and σ_{soil}^0 is due to bare soil interaction.

Using this WCM (Equation (1)), an AGWB training dataset, which was collected on the ground in four different years, 2006, 2011, 2012 and 2013 (Table 1), and the ALOS PALSAR imagery (HV polarization), Michelakis *et al.* in [42] undertook non-linear regression analysis to show that the HV intensity of the radar backscatter can be predicted in relation to the AGWB with an $R^2 = 0.92$ (Figure 4A).

Figure 4. (A) The non-linear regression model fitted (solid line) using the training dataset from Table 1 and ALOS PALSAR HV imagery; and (B) the histogram of both aboveground woody biomass (AGWB) datasets (training and external validation); note the zero AGWB points in scatterplot (A), which were collected on the ground using a global navigation satellite system (GNSS) device on areas with no woody vegetation to sample the backscatter in these areas.

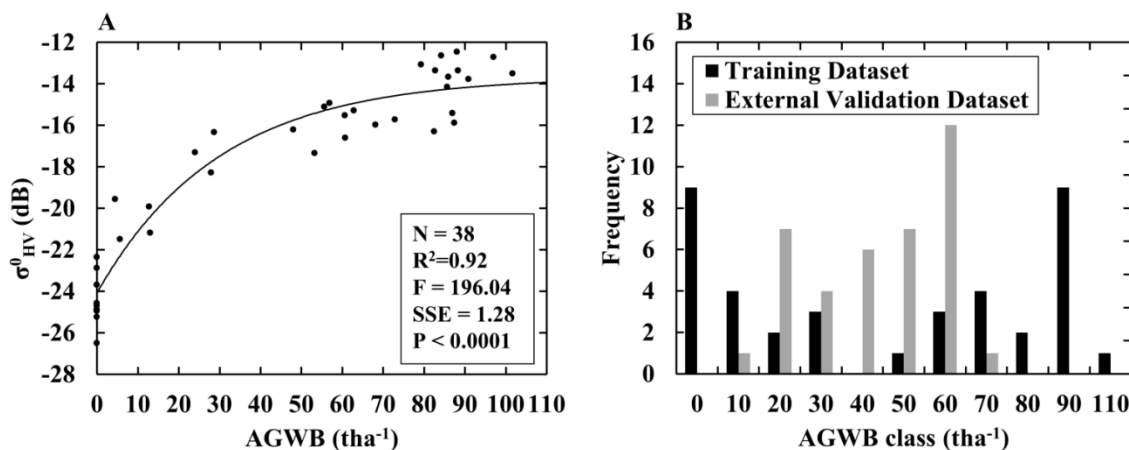


Table 1. Training and external validation AGWB datasets that were used in the non-linear regression fitting and the validation of the WCM; these datasets are described in [42].

Datasets	Plot size (ha)	AGWB (tha ⁻¹)			Density (Trees ha ⁻¹)			BA (m ² ha ⁻¹)		
		Range	Mean	St. Dev.	Range	Mean	SD	Range	Mean	St. Dev.
Training	32 × 1 6 × 0.1	0–101.6	47.3	37.1	0–680	155	171.7	0–15.3	6.15	5.0
Validation	38 × 0.1	1–72	39.5	19.4	20–350	145	75.1	0–11.0	5.7	2.6

Although the satellite data were collected in 2008, the slow growth rate of Caribbean pine, even in better sites in Belize as recorded by [45] (0.4 cm ≤ dbh ≤ 1 cm), allows us to use these field measurements in the development of the WCM. The semi-empirical model fitted in this study is shown

in Equation (3). Using an external validation dataset (Table 1), AGWB estimates were assessed demonstrating that AGWB can be predicted on the ground with a root mean squared error (RMSE) $\sim 13.5 \text{ tha}^{-1}$, while 80% of the AGWB estimates were found to have an error of less than 20 tha^{-1} [42].

$$\sigma_{HV}^0 = 10.40 \times (1 - e^{(-0.96 \times AGWB)}) - 24.06 \quad (3)$$

To assess the uncertainty of the AGWB map created using the ALOS PALSAR data and the semi-empirical WCM, an evaluation of the estimation accuracy was conducted using the validation dataset (Table 1) for the lower biomass range (*i.e.*, $\leq 75 \text{ tha}^{-1}$) and the training dataset (Table 1) for the higher biomass range (*i.e.*, $\geq 75 \text{ tha}^{-1}$). The training dataset was used for estimating uncertainty in the higher biomass range due to the lack of high biomass observations in the validation dataset. The relative root mean squared error (RRMSE) was separately calculated for seven biomass classes with 15 tha^{-1} intervals (*i.e.*, 0–15, 15–30, 30–45, 45–60, 60–75, 75–90 and 90–105 tha^{-1}) using Equation (4).

$$RRMSE (\%) = \left(100 \times \frac{RMSE}{\overline{AGWB}} \right) \quad (4)$$

where RMSE and \overline{AGWB} are the root mean squared error and the mean observed AGWB within each biomass class.

A concern with the mathematical formulation in Equation (2) is that negative or infinite values of biomass can be predicted [46–48]. To constrain estimates to realistic values, any cells with infinite values were assigned the highest value of biomass actually measured in the field (101.65 tha^{-1}), whilst any cells with negative estimates of biomass were assigned a value of zero. No previous field studies conducted in savanna woodlands in Belize by [45,49–52] have measured AGWB in these savanna woodlands above 101.65 tha^{-1} , so we feel confident using this value as our realistic upper limit for this case study.

Although a recent study from [53] has shown that parametric forward models show higher errors than other approaches, there are five reasons that a semi-empirical WCM is employed in this study: (1) The semi-empirical model is grounded in the physical basis of how the backscattered intensity of the radar is expected to interact with vegetation targets in contrast to more statistically driven approaches, such as backward models; (2) the use of non-parametric models, such as machine learning algorithms, could not be implemented in this research, because of the lack of the significant data amounts that are needed (for example, [54] used more than 50 data samples for biomass mapping using decision trees classifiers); (3) the WCM accounts for the low canopy cover nature of the savanna woodlands (10%–65%) by using a weighting area fill factor ($(1 - e^{(-\gamma \times AGWB)})$) in the vegetation backscatter [53]; (4) the WCM varies as it interacts with vegetation of different biomass and supplements and extends upon previous quantitative analysis of radar backscatter as a surrogate measure of biomass [42,44]; and (5) the biomass estimation results can be comparable to future research using methods that are based on other forward models in contrast to solely statistical approaches.

2.4. Deriving Ground-Based Estimates of AGWB for Two Protected Areas

We used the inverted WCM (Equation (2)) described in the previous section and the ALOS PALSAR data covering two of the country’s largest savanna woodlands (Rio Bravo Conservation and Management Area (RBCMA) and Deep River protected area) to estimate the mean AGWB for the whole protected area extent and compared these with AGWB estimates calculated from previously published data [50,52]. These two protected areas are both over 10,000 ha and are typical locations and extents for sub-national scale UN-REDD+ projects [17].

In RBCMA, Brown *et al.* in [52] estimated mean carbon stock of 13.1 tCha⁻¹ for approximately 10,000 ha of savanna by developing new allometric equations, which predicted biomass carbon using tree attributes as independent variables that could be easily measured from aerial images. To develop the allometric equations, Brown *et al.* used an extensive ground dataset, which was collected by the destructive sampling of 51 pine trees, and then 77 image sample plots were used in three-dimensional very high spatial resolution aerial imagery to assist with the remote measurement of the tree attributes, which were used to estimate carbon stocks. To convert the carbon stock estimation by Brown *et al.* to biomass, we multiplied by a factor of two [55] (carbon is 50% of biomass), calculating a mean AGWB of 26.2 tha⁻¹ for RBCMA. In Deep River (DR), to estimate AGWB for approximately 3500 ha of savanna woodlands (31.60 tha⁻¹), we used 62 circular sample plots (0.1 ha), which were not used during the WCM training, and only 18 out of the 62 were used in the external validation of the WCM, in the denser woodland areas originally collected by [50] to support plans for sustainable timber extraction (Table 2).

Table 2. Summary of the plots that were collected in the denser woodland areas of Deep River (DR).

Data	Plot size (ha)	AGWB (t ha ⁻¹)			Density (Trees ha ⁻¹)			BA (m ² ha ⁻¹)		
		Range	Mean	SD	Range	Mean	SD	Range	Mean	SD
DR	62 × 0.1	2.25–76.19	31.60	17.78	20–350	121	70.40	0.5–11.25	6.15	2.54

To derive the mean AGWB value for both RBCMA and DR, for each tree, the AGWB was estimated using the allometric equations (Equations (5) and (6)) developed by [52] in RBCMA, where dbh is the diameter at breast height (1.3 m) and biomass is dry aboveground woody biomass in kilograms. More than 30% (2190 trees) of the field data measurements that are used in this study were collected within RBCMA, and more than 95% of the tree dbh measurements are within the range sampled by [52] (1–52.4 cm). The AGWB ha⁻¹ was estimated for each 0.1 ha sample plot by summing the AGWB of individual trees and multiplying the sum by a factor of 10 to extrapolate to the hectare.

Having obtained these “ground truth” estimates of mean AGWB ha⁻¹ for both protected areas, we then multiplied these up by the area of the RBCMA and the denser woodland areas of DR and compared these totals to those obtained by using a GIS to aggregate cells from the 100-m biomass map within the boundaries of the RBCMA and DR, respectively.

$$Pine\ Biomass_{Kg} = 0.0407 \times dbh^{2.4323} \tag{5}$$

$$\text{Oak Biomass}_{Kg} = \left(0.5 + \frac{25,000 \times dbh^{2.5}}{dbh^{2.5} + 246,872} \right) \times 2 \quad (6)$$

2.5. Classification of Savannas by Protection and Management Type

Approximately 25% of the lowland savannas in Belize are under some form of protection [36] and have been characterized as Category Ia, II, IV or VI, according to the International Union for Conservation of Nature (IUCN) classification system [56]. Using information acquired from land managers and published management plans [50,57–60], we examined the influence of land management in various protected savanna woodlands by comparing the biomass quantities predicted by our model. In unprotected savanna woodlands, the possibility of a management plan cannot be excluded. However, it was not possible to acquire management information for these savannas woodlands; thus, the unprotected areas are considered as not managed in this study. To allow the influence of both passive and active management to be explored, as well as the binary “protected-unprotected” dichotomy, we subdivided the study area into three protection and management groups using the information acquired by managers and the published management plans.

Approximately 40 km² of savanna woodlands found within the RBCMA and in the Bladen nature reserve were characterized as highly protected and passively managed areas (henceforth, PRPM). These areas have been managed mostly to promote biodiversity [57–60], while they have been classified as “strict nature reserve, Ia” and “habitat/species management area, IV” by the IUCN. Similarly, some 118 km² of savanna woodlands found in the Manatee and DR forest reserves were grouped as protected and actively managed (PRAM) areas, where timber is extracted sustainably [50], and both have been classified as “protected area with sustainable use of natural resources, VI” by the IUCN. Further areas, totalling approximately 595 km² of savanna woodlands, with no protection designations, were identified as unprotected (UPR) areas. The remaining 185 km² of protected areas for which we could not obtain reliable information about their management were not included in this analysis. Using GIS, we then overlaid the new biomass map upon the three forest management groups and calculated the biomass in mean AGWB ha⁻¹ for each of the three areas.

2.6. Comparing the New Mapping with National Level Carbon Stock Maps from Pantropical Data Sets

To conduct a comparison with our local biomass map (Michelakis biomass estimates henceforth MBE₁₀₀), two national-level carbon stock maps were acquired for Belize. These were the pantropical national-level carbon stock dataset (Baccini biomass estimates, henceforth BBE₅₀₀) produced by [17] and the benchmark national carbon data (Saatchi biomass estimates, henceforth SBE₁₀₀₀) produced by [18]. Both datasets are stored in a single tagged image format file (*.tiff) representing the aboveground carbon density of aboveground live woody vegetation. These gridded values were predicted using data collected by a range of EO sensors, such as the ICESAT GLAS, MODIS and the Shuttle Radar Topography Mission (SRTM) in non-parametric spatial modelling processes. Baccini *et al.* used in [17] the RandomForests algorithm to produce the BBE₅₀₀ product, and Saatchi *et al.* in [18] used the Maximum Entropy (MaxEnt) modelling algorithm for the SBE₁₀₀₀ product [18]. The BBE₅₀₀ data were downloaded from the Woods Hole Research Centre (WHRC)

website [61] with a pixel size of 463.31 m \times 463.31 m, and the SBE₁₀₀₀ data were downloaded by [62] with a pixel size of 910.89 m \times 910.89 m.

To enable a cell-by-cell comparison between MBE₁₀₀, BBE₅₀₀ and SBE₁₀₀₀ at the 500-m and 1000-m scale using ANOVA and to produce percentage difference maps, we reduced the resolution of the MBE₁₀₀ data to 500 m and 1000 m, and the BBE₅₀₀ data from [61] to 1000 m (Table 3). We compared MBE₁₀₀ to both BBE₅₀₀ and BBE₁₀₀₀, to enable, in the first instance, a more direct comparison to the pantropical national carbon stock, using the spatial resolution defined by Baccini *et al.*, and at the former instance, to compare all three carbon maps at the coarser resolution (*i.e.*, 1000 m defined by Saatchi *et al.*). The data meaning for each reduced resolution pixel is the arithmetic mean of all the increased resolution pixel values, which were contained within the extent of each new reduced resolution pixel. To assess the differences between our local biomass estimates and these national carbon stock estimates, within the boundaries of our study area, we aggregated and averaged the grid values of our MBE₁₀₀ data set using a window size of 5 \times 5 and 10 \times 10 to create reduced resolution rasters (MBE₅₀₀, and MBE₁₀₀₀, respectively).

Table 3. Local and pantropical datasets used for comparison and summary of the data and methods used to derive the biomass maps; MBE, Michelakis biomass estimates; BBE, Baccini biomass estimates; SBE, Saatchi biomass estimates.

Biomass map	EO data used	Algorithm	Pixel size (m)	Reduced resolution (m)	Compared to
MBE ₁₀₀	ALOS PALSAR	Semi-empirical water cloud model	100	500	BBE ₅₀₀
				1000	BBE ₁₀₀₀ SBE ₁₀₀₀
BBE ₅₀₀	ICESAT GLAS MODIS Bidirectional Reflectance Distribution Function BDRF SRTM	RandomForests	500	1000	MBE ₅₀₀
					SBE ₁₀₀₀
SBE ₁₀₀₀	ICESAT GLAS MODIS LAI/NDVI/Vegetation Continuous Fields VCT SRTM QUICKSAT	MaxEnt	1000	-	MBE ₁₀₀₀
					BBE ₁₀₀₀

To perform AGWB comparisons between our reduced resolution AGWB estimates and BBE₅₀₀ and SBE₁₀₀₀ estimates, we calculated the percentage differences (Equation (7)) per pixel and per protected areas (*i.e.*, DR and RBCMA). To assess the difference between mean biomass estimations for the whole protected areas, percentage errors were calculated (Equation (8)).

In Equation (7), AGWB₁ and AGWB₂ refer to (1) the AGWB values in each individual pixel of the compared datasets (e.g., MBE₅₀₀ vs. BBE₅₀₀) or (2) the mean AGWB values derived using all biomass pixels of the compared datasets within the extent of a protected area. In Equation (8), AGWB_{reference} corresponds to the locally derived mean AGWB value for the woody savannas using field data in DR (Table 2) or to the derived mean AGWB calculated by [52] in BCMA. In Equation (8), AGWB_{estimated} refers to the AGWB estimates based on the MBE, BBE and SBE maps.

$$\text{Percentage Difference} = \frac{|AGWB_1 - AGWB_2|}{0.5 \times (AGWB_1 + AGWB_2)} \times 100 \quad (7)$$

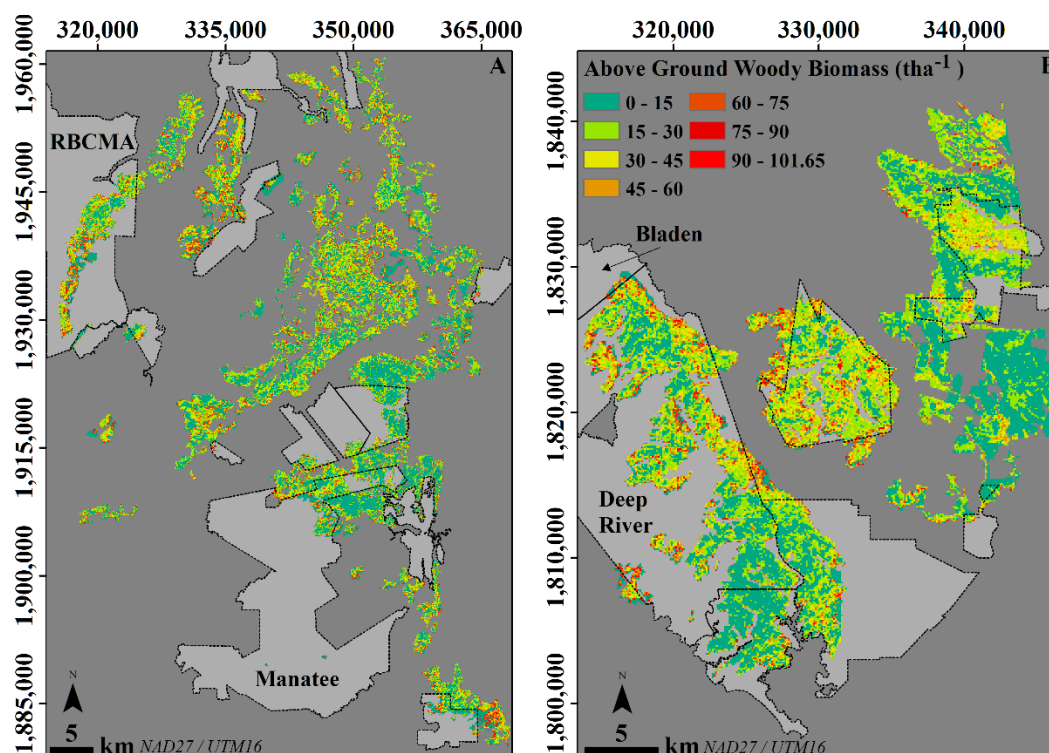
$$\text{Percentage Error} = \left| \frac{AGWB_{reference} - AGWB_{estimated}}{AGWB_{reference}} \right| \times 100 \quad (8)$$

3. Results and Discussion

3.1. Evaluating the AGWB of the Lowland Savannas per Protection and Management

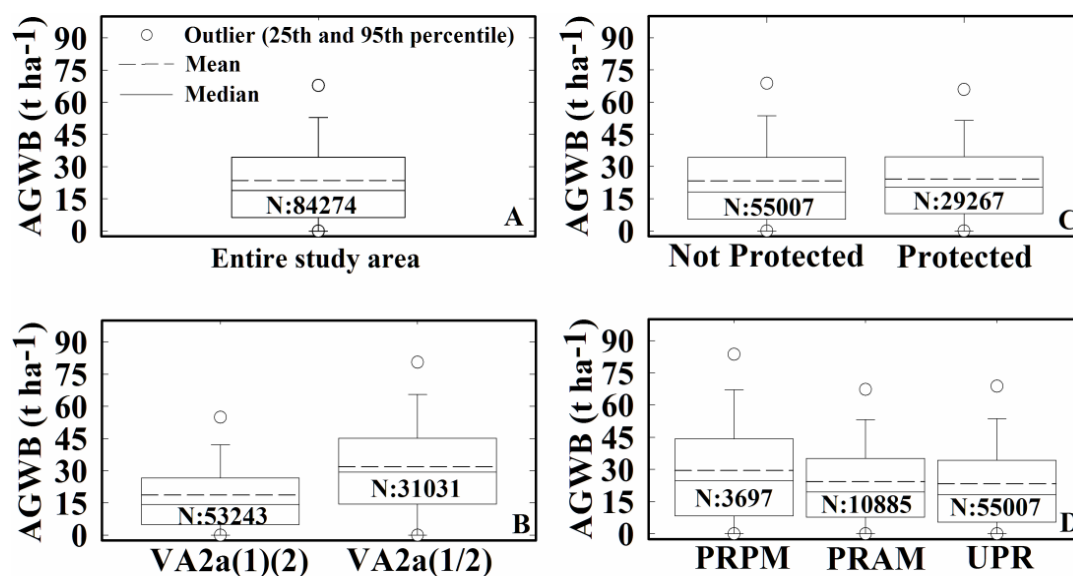
Using the semi-empirical model developed by [42], we create a 100-m biomass map (MBE_{100}) for the whole study area (Figure 5A,B). For the half of the total savanna area of the RBCMA that is covered by the ALOS PALSAR scene, we estimate mean AGWB based on 3,632 pixels from MBE_{100} to be $29.55 \pm 0.84 \text{ tha}^{-1}$, where the 95% confidence interval is reported with (\pm), and for the denser woodland areas sensed in the DR forest reserve (Figure 1D), $38.03 \pm 0.92 \text{ tha}^{-1}$ based on 3105 pixels. On average, slightly higher biomass values (mean AGWB = $24.18 \pm 0.24 \text{ tha}^{-1}$) were mapped within the boundaries of all of the protected areas in the study area compared to values mapped in other areas, which are considered unprotected ($23.29 \pm 0.19 \text{ tha}^{-1}$). Although this small difference in biomass is statistically significant (Mann–Whitney U -test, $p < 0.050$), the dispersion of biomass values in Figure 6C appears similar for both groups. Perhaps surprisingly, this suggests that protection in general does not lead to substantially higher values of mean AGWB ha^{-1} in these woodlands.

Figure 5. AGWB estimates (MBE_{100}) derived by ALOS PALSAR Scenes I, and II for (A) north Belize (Scene I) and (B) south Belize (Scene II), overlaid on protected areas boundaries (light grey polygons with dashed lines as boundaries) that contain savannas.



To explore this finding further, in Figure 6D, only the biomass values mapped within two types of protected areas are presented: those which are passively managed (PRPM) and those which are actively managed (PRAM); these are compared again to values mapped in unprotected areas (UPR). Differences in biomass are now more evident, and although the differences are again small, they are more significant (Kruskal–Wallis one-way ANOVA, $p < 0.001$). The protected areas that are passively managed (PRPM) with fire control and conservation management are estimated to have a mean AGWB of approximately $29.5 \pm 0.85 \text{ t ha}^{-1}$ and a higher variability of biomass values in comparison to protected areas that are actively managed for extractive logging (PRAM); for these latter areas, AGWB is estimated at approximately $24.3 \pm 0.41 \text{ t ha}^{-1}$, and the variability in the biomass values is lower. One possible explanation for this difference is that larger trees are commonly retained in biodiversity reserves, but are usually harvested before reaching such a size in forest reserves [50].

Figure 6. ALOS PALSAR-derived AGWB ha^{-1} estimates for (A) the study area (933 km^2), (B) the two UNESCO savanna land cover classes, (C) protected *versus* unprotected areas and (D) the protected areas with active management (PRAM), passive management (PRPM) and unprotected areas (UPR); in each case, N represents the number of pixels (104 m \times 104 m) from the biomass map falling within each of the groupings.



3.2. Using the Map to Characterize AGWB in the Lowland Savannas of Belize

Visual interpretation of the AGWB map (Figure 5A,B) indicates that the study areas are dominated by low mean AGWB ha^{-1} (0–30 t ha^{-1}). Analysis of the data shows that over 90% of the pixels show AGWB below 60 t ha^{-1} , with less than 10% of the remaining values predicted in the upper range from 60 t ha^{-1} to 101.65 t ha^{-1} (Figure 6A). The results obtained show that when AGWB is summed within the areas of the two UNESCO savanna classes mapped, each class produces almost the same total AGWB (VA2a (1) (2): 1.00 Mt; and VA2a (1/2): 0.99 Mt); however, the less dense UNESCO class VA2a (1) (2) covers some two-thirds of the study area. In Figure 6B, the denser VA2a (1/2) class is shown to contain significantly higher mean values of AGWB ha^{-1} ($\sim 32 \pm 0.27 \text{ t ha}^{-1}$ in comparison to $\sim 19 \pm 0.16 \text{ t ha}^{-1}$), a difference that is statistically significant (Mann–Whitney U statistic, $p < 0.001$).

The observed higher mean biomass found in VA2a (1/2) can be explained by the denser woody component being more extensively found in this class; in general, increasing number of trees ha⁻¹ has been found to produce increased mean AGWB ha⁻¹ in these savanna woodlands [42] and in other tropical savannas that are resource limited [26]. AGWB values estimated within the VA2a (1/2) vegetation class also showed a greater standard deviation (24.65 tha⁻¹ in comparison to 18.57 tha⁻¹). Taken together, these findings suggest that the less extensive VA2a (1/2) areas may be important to focus upon for carbon sequestration, and if they also have greater structural diversity, they may also be suitable for biodiversity conservation initiatives.

The RRMSE and the average estimated uncertainty of the AGWB mapping for each of the seven AGWB classes mentioned in Section 2.3 are shown in Table 4. The RRMSE for the lower AGWB classes (0–15 tha⁻¹ and 15–30 tha⁻¹) is considerably higher (113% and 78% respectively) in contrast to the RRMSE calculated (19%–52%) for the higher AGWB classes (30–105 tha⁻¹). Although the lower AGWB classes show considerable average uncertainty estimates (6.75 tha⁻¹ and 17.21 tha⁻¹), 80% of the uncertainty estimates for the MBE₁₀₀ pixels (Figure 7) are lower or close to 20 tha⁻¹ (Table 4).

Figure 7. Uncertainty estimates for MBE₁₀₀ derived by ALOS PALSAR for (A) north Belize (Scene I) and (B) south Belize (Scene II), overlaid on protected area boundaries (light grey polygons with dashed lines as boundaries) that contain savannas.

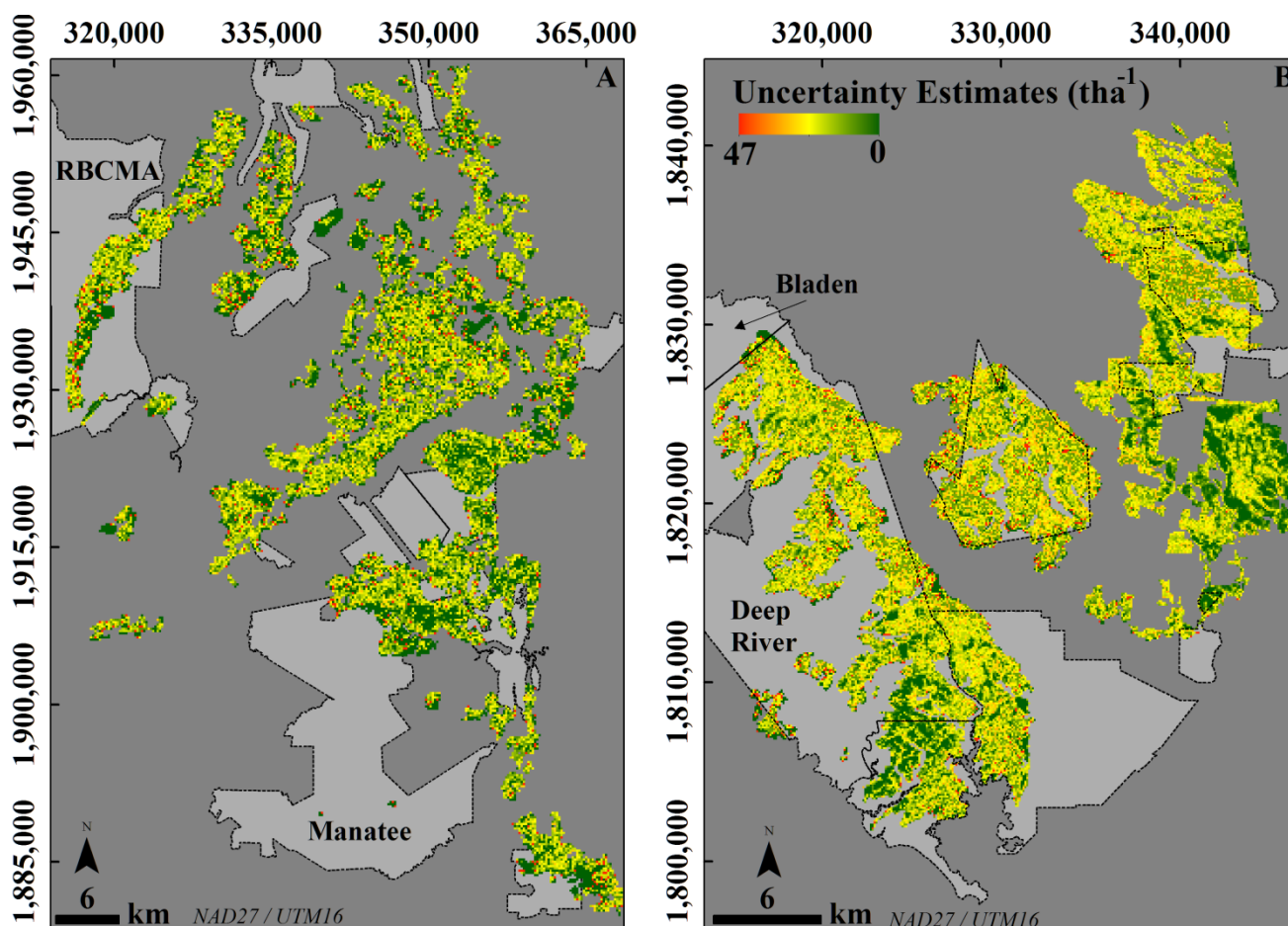


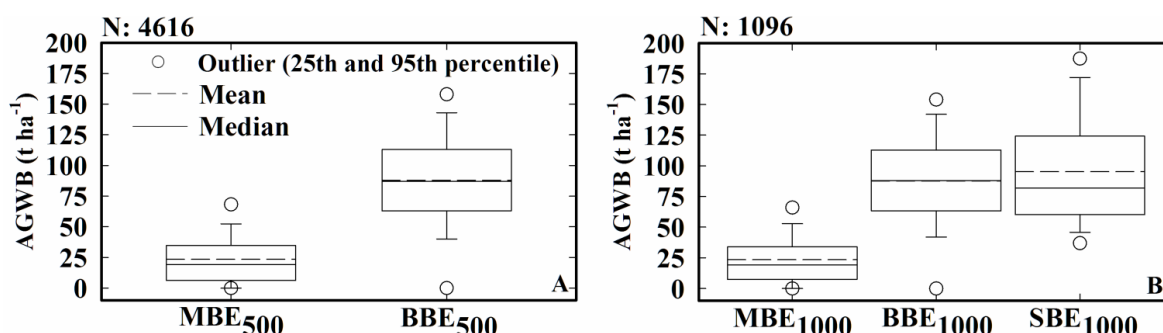
Table 4. Estimated uncertainty values and their basic description per AGWB class; letters T and V indicate the dataset that was used in the RMSE and average AGWB calculations (*i.e.*, T, training, or V, validation); note that 13 observations of AGWB (*i.e.*, $\geq 75 \text{ tha}^{-1}$) are used from the training dataset to calculate uncertainty for the higher AGWB classes.

AGWB Class (tha^{-1})	Number of AGWB Observations	Average AGWB Observed (tha^{-1})	Estimated Uncertainty (tha^{-1})					
			RMSE (tha^{-1})	RRMSE (%)	Number of MBE ₁₀₀ Pixels	Average (tha^{-1})	Max (tha^{-1})	80th Percentile (tha^{-1})
0–15	4 (V)	10.84	14.2	131	35,425	6.75	19.64	14.21
15–30	8 (V)	20.60	16.02	78	22,758	17.21	23.40	20.67
30–45	11 (V)	38.88	7.43	19	13,774	6.96	8.55	7.79
45–60	9 (V)	51.98	15.13	29	6247	14.93	17.40	16.48
60–75	6 (V)	66.30	14.62	22	3014	14.66	16.50	15.64
75–90	10 (T)	85.10	43.8	51.47	1489	42.00	45.90	43.86
90–105	3 (T)	96.51	25.58	26.51	1567	26.81	27.45	27.45

3.3. Comparison of the Local Map Estimates with Pantropical Carbon Stock Maps

The reduced resolution rasters MBE₅₀₀, and MBE₁₀₀₀ derived in Section 2.6 contain pixels with the arithmetic mean of the input pixels (MBE₁₀₀). Based on 4616 pixels (pixel size: 500 m), it is evident from Figure 8A that BBE₅₀₀ predicts significantly higher mean AGWB ha^{-1} for the whole study area than MBE₅₀₀ ($\sim 88 \pm 1.21 \text{ tha}^{-1}$ vs. $\sim 24 \pm 0.632 \text{ tha}^{-1}$; percentage difference = +115.50%).

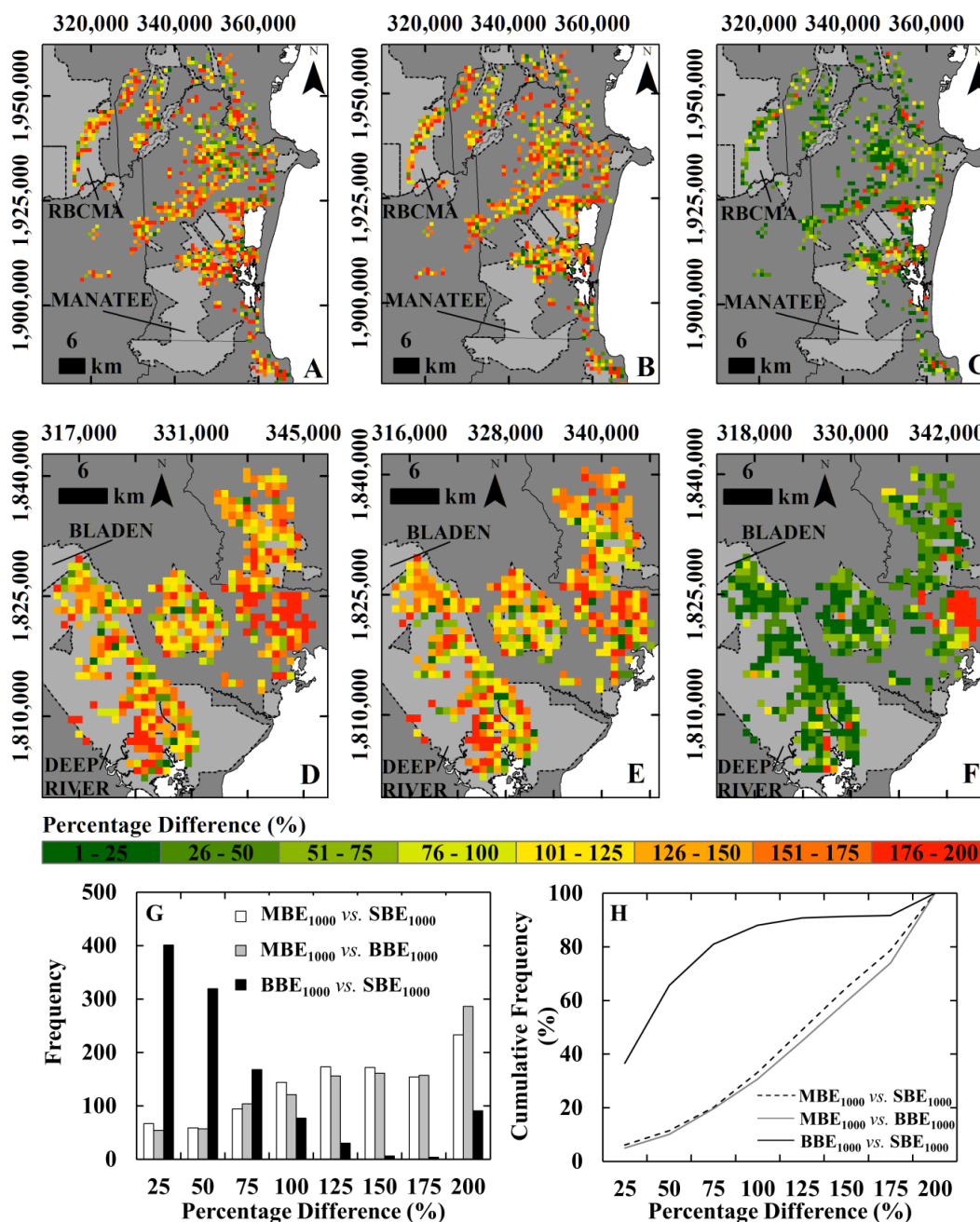
Figure 8. Differences between biomass maps for (A) 500-m and (B) 1000-m resolution.



Based on 1096 pixels of 1000-m pixel size (Figure 8B), the SBE₁₀₀₀ AGWB estimation ($\sim 95 \pm 2.86 \text{ tha}^{-1}$) is higher than both the BBE₁₀₀₀ and MBE₁₀₀₀ ($\sim 88 \pm 2.50 \text{ tha}^{-1}$ and $\sim 24 \pm 1.28 \text{ tha}^{-1}$, respectively) (percentage diff. = +8.2% and +121%, respectively). A Kruskal–Wallis ANOVA test ($p \leq 0.001$) and percentage difference maps (Figure 9A–F) using pixel-by-pixel comparisons confirm that the 500-m and 1000-m biomass maps yield significantly different and higher biomass estimates compared to those from aggregating our 100-m estimates ($p \leq 0.001$). The relatively similar magnitudes of the estimates for the two pantropical carbon maps produced by [17,18] is expected (Figure 9 C,F), since they have used very similar EO data and allometric equations to derive biomass

estimations, with the main difference being only the machine learning algorithm used (RandomForests, versus MaxEnt, respectively).

Figure 9. Percentage differences as calculated from Equation (7) per 1000-m pixel for the comparisons between (A,D) MBE₁₀₀₀ vs. BBE₁₀₀₀, (B,E) MBE₁₀₀₀ vs. SBE₁₀₀₀ and (C,F) BBE₁₀₀₀ vs. SBE₁₀₀₀ for northern and southern Belizean savannas within the ALOS PALSAR scenes; in histogram (G), we show the distribution of the percentage differences pixel-wise for each biomass map comparison group, and in scatterplot (H), we show the relationship between the percentage difference for each pixel and the biomass estimated for the same pixel using the MBE₁₀₀₀ maps.



Whilst the above comparison was done for the entire study area to maximize the data volume included, we also compared the estimates from the different biomass maps for the RBCMA and DR

areas, since these are more typical of the areas of interest to land managers in Belize. We found that the carbon stock maps created for RBCMA and DR using data from [17,18] at 1-km spatial resolution again produced significant overestimation of the mean AGWB ha^{-1} compared to local reference values from the field surveys described earlier. Percentage errors were 277% and 319% for BBE_{1000} and SBE_{1000} , respectively, in the RBCMA and 302% and 298% for BBE_{1000} and SBE_{1000} , respectively, in DR. In contrast, upscaling our finer scale AGWB estimations in both the RBCMA and DR did not produce large overestimation compared to the same local reference values (+8.1% and +4.5%, respectively, for MBE_{500} and 10.7% and 0.04% for the MBE_{1000}). Similar findings are observed in [63], where Hill *et al.* find considerable differences in mean AGWB by comparing between the biomass maps produced by [23] and [17] for a small study area in Mozambique ($\sim 1160 \text{ km}^2$), which is dominated by Miombo woodlands (mean AGWB $\sim 35.6\text{--}38.4 \text{ tha}^{-1}$ found in [23] *vs.* 102.4 tha^{-1} found in [17]). These findings confirm the need for caution when using biomass estimations produced from satellite EO [63] at coarse resolution for quantifying AGWB locally.

Generally, these estimates of AGWB by our local method ($\sim 26 \text{ tha}^{-1}$) and by the pantropical data sets ($\sim 90 \text{ tha}^{-1}$) need to be considered in the context of the ranges of aboveground biomass that are estimated for woody savannas in other parts of the world. According to a review of observations by [1], the highest values of biomass observed in savannas have been in Northern Australia ($\sim 67.2 \text{ tha}^{-1}$) [64], while in South and Central America, the highest biomass values recorded have been observed in Brazilian cerrado vegetation ($\sim 31.8 \text{ tha}^{-1}$) [65]. This leads to the suggestion that the pantropical carbon maps may be overestimating AGWB in savanna areas, and this suggestion will need to be explored more rigorously as more field-based estimates of biomass are collated from other savanna woodlands.

4. Conclusions

This study has shown that ALOS PALSAR radar data can be used with semi-empirical modelling to produce estimates of AGWB ha^{-1} for the woody component of tropical savannas at a spatial resolution of 100 m. When these pixel estimates are aggregated within the extents of two protected areas of approximately 10,000 ha, the satellite-derived biomass maps agree to within 12% and 20%, respectively, of the estimates obtained from local forest survey data and from biomass estimated from airborne very high spatial resolution imagery, suggesting that this method has sufficient accuracy to be used for reporting biomass estimates for sub-national extents.

Over 90% of the woodlands mapped in Belize are estimated to have an AGWB less than 60 tha^{-1} , and the average woody biomass of these savannas is estimated at $\sim 23.5 \text{ tha}^{-1}$. Overlaying the results upon previous thematic mapping of national land cover allows us to assign a representative mean biomass value of $\sim 32 \text{ tha}^{-1}$ to UNESCO savanna class VA2a (1/2) (“denser tree savanna”), which clearly separates it from the “less dense” VA2a (1) (2) land cover variant ($\sim 18 \text{ tha}^{-1}$). This is the first quantitative assessment of the difference in the woody component between these two land cover classes, and this information significantly enhances the value of the existing land cover map for forest managers.

A two-way comparison of the mean AGWB values mapped for all protected *versus* all unprotected areas in the study area showed a small gain in biomass within protected areas; further subdivision of

the protected areas revealed higher AGWB values ($\sim 30 \text{ tha}^{-1}$) for passively managed biodiversity reserves than for the extractive forest reserves ($\sim 25 \text{ tha}^{-1}$).

The comparison of our AGWB estimate to the pantropical carbon stock maps produced by Baccini *et al.* in [17] and Saatchi *et al.* in [18] shows that the three biomass estimates are not consistent, with both pantropical data sets significantly overestimating AGWB when compared to estimations based on more localized backscatter-biomass relationships constrained by forest survey data. The evidence from this study suggests that the pantropical carbon stock maps overestimate the biomass of savanna woodlands in Belize at the national level and are also less suited for exploring differences in AGWB at the sub-national scale, for example for monitoring biomass differences within and between the country's protected areas.

Acknowledgments

This work is supported by a Hellenic Scholarships Foundation (IKY) Scholarship from the resources of Operational Programme (O.P.) “Education and Lifelong Learning”, the European Social Fund (ESF) and the National Strategic Reference Framework (NSRF) 2007–2013, as well as by the School of Geosciences of the University of Edinburgh. We are grateful to the Darwin Initiative project, “Savannas Ecosystem Assessment/Belize 2009–2012, and the Environmental Research Institute of the University of Belize for providing logistical help and resources for the collection of the field data. We wish to thank Planet Action for providing the satellite data used to identify the field data collection sites and the Institute of Geography Centenary Fund for providing part of the funding for the fieldwork component. We are particularly grateful to the forestry team of the NGO “Programme for Belize” and the students of the MSc in Plant Taxonomy organized by the Royal Botanical Gardens of Edinburgh for their assistance with collecting field data in the Rio Bravo Conservation and Management Area. We wish to thank the four anonymous reviewers for their constructive suggestions, which significantly improved this manuscript.

Author Contributions

Dimitrios Michelakis, Neil Stuart and Iain H. Woodhouse conceived and designed the experiments; Dimitrios Michelakis performed the experiments; and analyzed the data; German Lopez and Vinicio Linares contributed reagents/materials/analysis tools; Dimitrios Michelakis wrote the paper.

Conflicts of Interest

The authors declare no conflict of interest.

References and Notes

1. Grace, J.; José, J.S.; Meir, P.; Miranda, H.S.; Montes, R.A. Productivity and carbon fluxes of tropical savannas. *J. Biogeogr.* **2006**, *33*, 387–400.
2. Ratnam, J.; Bond, W.J.; Fensham, R.J.; Hoffman, W.A.; Archibald, S.; Lehmann, C.E.R.; Anderson, M.T.; Higgins, S.I.; Sankaran, M. When is a ‘forest’ a savannas, and why does it matter? *Glob. Ecol. Biogeogr.* **2011**, *20*, 653–660.

3. FAO. *Global Forest Resources Assessment, Main Report*; Food and Agriculture Organization of the United Nations: Rome, Italy, 2010.
4. Furley, P. Tropical savannas: Biomass, plant ecology, and the role of fire and soil on vegetation. *Progr. Phys. Geogr.* **2010**, *34*, 563–585.
5. Castro, E.A.; Kauffman, J.B. Ecosystem structure in the Brazilian Cerrado: A vegetation gradient of aboveground biomass, root mass and consumption by fire. *J. Trop. Ecol.* **1998**, *14*, 263–283.
6. Felipe, J.; Ribeiro, F.; Ratter, A.J.; Bridgewater, S. *Neotropical Savannas and Seasonally Dry Forests Plant Diversity, Biogeography, and Conservation*; Pennington, T.R., Gwilym, P.L., Ratter, A.J., Eds.; CRC Press: Boca Raton, FL, USA, 2006.
7. Klink, C.A.; Machado, R.B. Conservation of the Brazilian Cerrado. *Conserv. Biol.* **2005**, *19*, 707–713.
8. UN Collaborative Programme on Reducing Emissions from Deforestation and Forest Degradation in Developing Countries (UN-REDD)-Framework Document. Available online: <http://www.un-redd.org/> (accessed on 24 September 2014).
9. Ratter, J.A.; Ribeiro, J.F.; Bridgewater, S. The Brazilian Cerrado vegetation and threats to its biodiversity. *Ann. Bot.* **1997**, *80*, 223–230.
10. Silva, J.M.C.; Bates, J.M. Biogeographic Patterns and Conservation in the South American Cerrado: A Tropical Savannas Hotspot. *BioScience* **2002**, *52*, 225–234.
11. Frost, P.G.H.; Robertson, F. The ecological effects of fire in savannas. *IUBS Monogr. Series* **1985**, *3*, 93–140.
12. Hannan, N.P.; Sea, W.B.; Dangelmayr, G.; Govender, N. Do Fires in Savannas Consume Woody Biomass? A Comment on Approaches to Modeling Savannas Dynamics. *Am. Nat.* **2008**, *171*, 6.
13. Lehmann, C.E. Savannas need protection. *Science* **2010**, *327*, 642–643.
14. Bond, W.J. What Limits Trees in C4 Grasslands and Savannas? *Annu. Rev. Ecol. Evol. Syst.* **2008**, *39*, 641.
15. Gibbs, H.; Brown, S.; Niles, J.; Foley, J. Monitoring and estimating tropical forest carbon stocks: Making REDD a reality. *Environ. Res. Lett.* **2007**, *2*, 4.
16. Silva, J.M.N.; Carreiras, J.M.B.; Rosa, I.; Pereira, J.M.C. Greenhouse gas emissions from shifting cultivation in the tropics, including uncertainty and sensitivity analysis. *J. Geophys. Res. Atmos.* **2011**, *116*, D20.
17. Baccini, A.; Goetz, S.J.; Walker, W.S.; Laporte, N.T.; Sun, M.; Sulla-Menashe, D.; Hackler, J.; Beck, P.S.A.; Dubayah, R.; Friedl, M.A.; Samanta, S.; Houghton, R.A. Estimated carbon dioxide emissions from tropical deforestation improved by carbon-density maps. *Nat. Clim. Chang.* **2012**, *2*, 182–185.
18. Saatchi, S.S.; Harris, L.H.; Brown, S.; Lefsky, M.; Mitchard, E.T.A.; Salas, W.; Zutta, B.R.; Buermann, W.; Lewis, S.L.; Hagen, S.; Petrova, S.; White, L.; Silman, M.; Morel, A. Benchmark map of forest carbon stocks in tropical regions across three continents. *Proc. Natl. Acad. Sci. USA* **2011**, *108*, 9899–9904.
19. Zeng, T.; Dong, X.; Quegan, S.; Hu, C.; Uryu, Y. Regional tropical deforestation detection using ALOS PALSAR 50 m mosaics in Riau province, Indonesia. *Electron. Lett.* **2014**, *50*, 547–549.
20. Shimada, M.; Tadono, T.; Rosenqvist, A. Advanced Land Observing Satellite (ALOS) and Monitoring Global Environmental Change. *Proc. IEEE* **2010**, *98*, 780–799.

21. De Grandi, D.G.; Bouvet, A.; Lucas, M.R.; Shimada, M.; Monaco, S.; Rosenqvist, A. The K&C PALSAR Mosaic of the African Continent: Processing Issues and First Thematic Results. *IEEE Trans. Geosci. Remote Sens.* **2011**, *49*, 3593–3610.
22. Mitchard, E.T.A.; Saatchi, S.S.; Woodhouse I.H.; Nangendo, G.; Ribeiro, N.S.; Williams, M.; Ryan, C.M.; Lewis, S.L.; Feldpausch, T.R.; Meir, P. Using satellite radar backscatter to predict above-ground woody biomass: A consistent relationship across four different African landscapes. *Geophys. Res. Lett.* **2009**, *36*, 23.
23. Ryan, C.M.; Hill, T.; Woollen, E.; Ghee, C.; Mitchard, E.; Cassells, G.; Grace, J.; Woodhouse, I.; Williams, M. Quantifying small-scale deforestation and forest degradation in Miombo woodlands using high-resolution multi-temporal radar imagery. *Glob. Chang. Biol.* **2011**, *18*, 243–257.
24. Lucas, R.M.; Armston, J.D. ALOS PALSAR for characterizing wooded savannas in Northern Australia. In Proceedings of the Geoscience and Remote Sensing Symposium, 2007 IEEE International, IGARSS, Barcelona, Spain, 23–28 July 2007; pp. 3610–3613.
25. Woodhouse, I.H.; Mitchard, E.T.A.; Brolly, M.; Maniatis, D.; Ryan, C.M. Radar backscatter is not a ‘direct measure’ of forest biomass. *Nat. Clim. Chang.* **2012**, *2*, 556–557.
26. Cassells, G.F.; Woodhouse, I.H.; Mitchard, E.T.A.; Tembo, M.D. The use of ALOS PALSAR for supporting sustainable forest use in southern Africa: A case study in Malawi. In Proceedings of the Geoscience and Remote Sensing Symposium, 2009 IEEE International, IGARSS, Cape Town, South Africa, 12–17 July 2009; Volume 2, pp. 206–209.
27. Jantz, P.; Goetz, S.; Laporte, N. Carbon stock corridors to mitigate climate change and promote biodiversity in the tropics. *Nat. Clim. Chang.* **2014**, *4*, 138–142.
28. Banfai, D.S.; Bowman, D.M. Dynamics of a savannas-forest mosaic in the Australian monsoon tropics inferred from Stand structures and historical aerial photography. *Aust. J. Bot.* **2005**, *53*, 185–194.
29. Hennenberg, K.J.; Fischer, F.; Kouadio, K.; Goetze, D.; Orthmann, B.; Linsenmair, K.E.; Jeltsch, F.; Porembski, S. Phytomass and fire occurrence along forest-savannas transects in the Comoe National Park, Ivory Coast. *J. Trop. Ecol.* **2006**, *22*, 303–311.
30. House, J.I.; Archer, S.; Breshears, D.D.; Scholes, R.J. Conundrums in mixed woody-herbaceous plant systems. *J. Biogeogr.* **2003**, *30*, 1763–1777.
31. Woollen, E.; Ryan, C.; Williams, M. Carbon Stocks in an African Woodland Landscape: Spatial Distributions and Scales of Variation. *Ecosystems* **2012**, *15*, 804–818.
32. Furley, P.A.; Rees, R.; Ryan, C.; Saiz, G. Savannas burning and the assessment of long-term fire experiments with particular reference to Zimbabwe. *Progr. Phys. Geogr.* **2008**, *32*, 611–634.
33. Furley, P.A. Tropical savannas and associated forests: Vegetation and plant ecology. *Progr. Phys. Geogr.* **2007**, *31*, 203–211.
34. Lucas, R.M.; Cronin, L.; Moghaddam, M.; Lee, A.; Armston, J.; Bunting, P.; Witte, C. Integration of radar and Landsat-derived foliage projected cover for woody regrowth mapping, Queensland, Australia. *Remote Sens. Environ.* **2006**, *100*, 388–406.
35. Clewley, D.; Lucas, R.; Accad, A.; Armston, J.; Bowen, M.; Dwyer, J.; Pollock, S.; Bunting, P.; McAlpine, C.; Eyre, T.; Kelly, A.; Carreiras, J.; Moghaddam, M. An Approach to Mapping Forest Growth Stages in Queensland, Australia through Integration of ALOS PALSAR and Landsat Sensor Data. *Remote Sens.* **2012**, *4*, 2236–2255.

36. Bridgewater, S.; Cameron, I.; Furley, P.; Goodwin, Z.; Kay, E.; Lopez, G.; Meerman, J.; Michelakis, D.; Moss, D.; Stuart, N. *Savannas in Belize: Results of Darwin Initiative Project 17-022 and Implications for Savannas Conservation*; University of Edinburgh: Edinburgh, UK, 2012.
37. Bridgewater, S.G.M.; Ibanez, A.; Ratter, J.A.; Furley, P.A. Vegetation classification and floristics of the savannas and associated wetlands of Rio Bravo Conservation and Management Area, Belize. *Edinb. J. Bot.* **2002**, *59*, 421–442.
38. Mistry, J. *World Savannas: Ecology and Human Use*; Prentice Hall: London, UK, 2000; p. 344.
39. Furley, P.A.; Len thall, J.; Bridgewater, S. A phytogeographic analysis of the woody elements of New World savannas. *Edinb. J. Bot.* **1999**, *56*, 293–305.
40. Goodwin, Z.A.; Lopez, G.N.; Stuart, N.; Bridgewater, S.G.M.; Haston, E.M.; Cameron, I.D.; Michelakis, D.; Ratter, J.A.; Furley, P.A.; Kay, E.; *et al.* A checklist of the vascular plants of the lowland savannas of Belize, Central America. *Phytotaxa* **2013**, *101*, 1–119.
41. Meerman, J.; Sabido, W. Central American Ecosystems Map. Available online: http://biological-diversity.info/Downloads/Volume_Iweb_s.pdf (accessed on 31 March 2014).
42. Michelakis, D.G.; Stuart, N.; Brolly, M.; Woodhouse, I.H.; Lopez, G.; Linares, V. Estimation of Woody Biomass of Pine Savannas Woodlands from ALOS PALSAR Imagery. *IEEE J. Sel. Top. Appl. Earth Obs. Remote Sens.* 2014, accepted.
43. Michelakis, D.G.; Stuart, N.; Woodhouse, I.H.; Lopez, G.; Linares, V. Establishing the sensitivity of ALOS PALSAR to aboveground woody biomass: A case study in the pine savannas of Belize, Central America. In Proceedings of the Geoscience and Remote Sensing Symposium, 2013 IEEE International, IGARSS, Melbourne, VIC, Australia, 21–26 July 2013; pp. 953–956.
44. Attema, E.P.W.; Ulaby, F.T. Vegetation modeled as a water cloud. *Radio Sci.* **1978**, *13*, 357–364.
45. Johnson, M.S. *An Inventory of the Southern Coastal Plain Pine Forests, Belize*; Ministry of Overseas Development, Land Resources Division: Surrey, UK, 1974.
46. Magnusson, M.; Fransson, J.E.S.; Eriksson, L.E.B.; Sandberg, G.; Smith-Jonforsen, G.; Ulander, L.M.H. Estimation of forest stem volume using ALOS PALSAR satellite images. In Proceedings of the Geoscience and Remote Sensing Symposium, 2007 IEEE International, IGARSS, Barcelona, Spain, 23–28 July 2007; pp. 4343–4346.
47. Peregon, A.; Yamagata, Y. The use of ALOS/PALSAR backscatter to estimate above-ground forest biomass: A case study in Western Siberia. *Remote Sens. Environ.* **2013**, *137*, 139–146.
48. Askne, J.; Santoro, M.; Smith, G.; Fransson, J. Multitemporal Repeat-Pass SAR Interferometry of Boreal Forests. *IEEE Trans. Geosci. Remote Sens.* **2003**, *41*, 1540–1550.
49. Viergever, K.; Woodhouse, I.H.; Stuart, N. Backscatter and interferometry for estimating above-ground biomass in tropical savannas woodland. In Proceedings of the Geoscience and Remote Sensing Symposium, 2009 IEEE International, IGARSS, Cape Town, South Africa, 12–17 July 2009; pp. 2346–2349.
50. Linares, V. Sustainable forest management plan Deep River forest reserve 2009. Available online: http://pdf.usaid.gov/pdf_docs/PDACP774.pdf (accessed on 20 June 2014).
51. Michelakis, D.G.; Stuart, N.; Furley, P.A.; Lopez, G.; Linares, V.; Woodhouse, I.H. Structure and population density of pine savannas woodlands in Belize, Central America. *Caribb. J. Sci.* **2014**, submitted.

52. Brown, S.; Pearson, T.; Slaymaker, D.; Ambagis, S.; Moore, N.; Novelo, D.; Sabido, W. Creating a virtual tropical forest from three-dimensional aerial imagery to estimate carbon stocks. *Ecol. Appl.* **2005**, *15*, 1083–1095.
53. Tanase, M.A.; Panciera, R.; Lowell, K.; Tian, S.; Garcia-Martin, A.; Walker, J.P. Sensitivity of L-Band Radar Backscatter to Forest Biomass in Semiarid Environments: A Comparative Analysis of Parametric and Nonparametric Models. *IEEE Trans. Geosci. Remote Sens.* **2014**, *52*, 4671–4685.
54. Carreiras, M.B.J.; Melo, J.B.; Vasconcelos, M.J. Estimating the Above-Ground Biomass in Miombo Savannas Woodlands (Mozambique, East Africa) Using L-Band Synthetic Aperture Radar data. *Remote Sens.* **2013**, *5*, 1524–1548.
55. Schlesinger, W.H. *Biogeochemistry, an Analysis of Global Change*; Academic Press: New York, NY, USA, 1997.
56. Dudley, N. *Guidelines for Applying Protected Areas Management Categories*; IUCN: Gland, Switzerland, 2008; p. 86.
57. McLoughlin, L.; Hofman, M.; Ack, M. Protected Areas Management Program – Second Quarterly Report 2012. Available online: <http://www.yaaxche.org/files/PAM%20Q2%20Report%202012.pdf> (accessed on 31 March 2014).
58. McLoughlin, L.; Hofman, M.; Ack, M.; Chub, J. Protected Areas Management Program – Second Quarter Report, 2013. Available online: http://www.yaaxche.org/files/PAM_Q2_2013_Report.pdf (accessed on 31 March 2014).
59. McLoughlin, L.; Hofman, M.; Ack, M.; Chub, J. Protected Areas Management Program—Third Quarter Report, 2013. Available online: http://www.yaaxche.org/files/PAM_Q3_2013_Report.pdf (accessed on 31 March 2014).
60. Programme for Belize. *Rio Bravo Conservation and Management Area Sustainable Timber Programme-Forest Management Plan and Operational Guidelines*; Programme for Belize: Belize City, Belize, 2006.
61. Woods Hole Research Center. Available online: <http://www.whrc.org> (accessed on 31 March 2014).
62. Saatchi, S. Carbon Jet Propulsion Laboratory. Available online: ftp://www-radar.jpl.nasa.gov/projects/carbon/datasets/Americas/Belize/belize_agb/ (accessed on 27 June 2014).
63. Hill, T.C.; Williams, M.; Bloom, A.A.; Mitchard, E.T.A.; Ryan, C.M. Are Inventory Based and Remotely Sensed Above-Ground Biomass Estimates Consistent? *PLoS One* **2013**, *8*, e74170.
64. Chen, X.; Hutley, L.B.; Eamus, D. Carbon balance of tropical savannas of northern Australia. *Oecologia* **2003**, *137*, 405–416.
65. Abdala, G.C.; Caldas, L.S.; Haridasan, M.; Eiten, G. Above and belowground organic matter and root, shoot ratio in a cerrado in Central Brazil. *Braz. J. Ecol.* **1998**, *2*, 11–23.